Single-User and Multi-User MIMO Channel Estimation for LTE-Advanced Uplink

Stefan Pratschner*, Stefan Schwarz*† and Markus Rupp*
†Christian Doppler Laboratory for Dependable Wireless Connectivity for the Society in Motion
*Institute of Telecommunications, TU Wien, Austria
{spratsch,sschwarz,mrupp}@nt.tuwien.ac.at

***Abstract*—In LTE-Advanced (LTE-A) demodulation reference symbols are employed for pilot aided channel estimation to perform coherent detection. Since these reference symbols are allocated on the same time-frequency positions for all users in Multi-User MIMO (MU-MIMO) operation or for all spatial layers in Single-User MIMO (SU-MIMO), they are designed to be code-domain orthogonal in order to be separable at the receiver. This orthogonality is obtained by cyclically shifting a reference signal base sequence, where the specific cyclic shift values are signaled to each user. In this work we show formal equivalence of SU-MIMO and MU-MIMO for LTE-A uplink in the context of channel estimation. We propose a standard compliant mapping that assigns cyclic shifts to users such that SU-MIMO estimation methods are applicable also for MU-MIMO transmissions. Further we show the trade-off between the number of active users and the channel's frequency selectivity in MU-MIMO operation due to the residual channel estimation error.**

***Index Terms*—channel estimation, LTE-A, uplink, multi-user, MIMO**

I. Introduction

Channel estimation in 3rd Generation Partnership Project (3GPP) LTE-Advanced (LTE-A) is pilot aided, meaning that known reference symbols are multiplexed in the Orthogonal Frequency Division Multiplexing (OFDM) time-frequency resource grid to enable channel estimation at the receiver. In the LTE-A uplink two kinds of reference symbols, Sounding Reference Signal (SRS) and Demodulation Reference Signal (DMRS), are standardized [1]. While SRS are employed for channel sounding and for scheduling and feedback parameter estimation, we focus on channel estimation for the purpose of coherent detection utilizing DMRS in our work.

In order to save reference symbol overhead in Multiple-Input Multiple-Output (MIMO) transmissions, reference symbols of all spatial streams are allocated on the same time-frequency resources as illustrated in Fig. 1. Due to the overlapping reference symbol allocation, channel estimation in LTE-A uplink is significantly different from the downlink and was already considered by many others, in terms of Single-User MIMO (SU-MIMO) [2]–[5] as well as in the context of Multi-User MIMO (MU-MIMO) [3]–[10]. While most authors consider channel estimation in the time domain, which leads to Channel Impulse Response (CIR) leakage, only [8] and our previous work [11] consider estimation in the frequency domain, avoiding this problem.

In any case, code domain orthogonality of DMRS is exploited to separate estimated MIMO channels of different User Equipment (UE)s or different spatial transmission layers. This orthogonal structure is obtained by cyclic shifts of reference symbols which are signaled in terms of the Cyclic Shift Field (CSF) within the Downlink Control Information (DCI) to the user. Although equivalence of uplink SU-MIMO and MU-MIMO channel estimation is widely understood in theory, authors often do not consider constraints imposed by the standard. Since there are only three bits reserved within the DCI field for signaling of the CSF, at most eight users may be scheduled simultaneously. Further, a specific mapping between users and a corresponding cyclic shift value is necessary to ensure orthogonality between UEs in MU-MIMO which is not proposed by any other work to the best of the authors knowledge. Also, since a frequency selective channel destroys DMRS orthogonality in general, separation of estimated MU-MIMO channels is more difficult for strong multipath propagation. In such a scenario, the maximum applicable number of users for MU-MIMO is not limited by the number of CSF values, but by the channel's frequency selectivity for correlation based channel estimation.

In this paper, we show the equivalence of SU-MIMO and MU-MIMO in the LTE-A uplink for channel estimation. We explain how code domain orthogonality between reference symbols of different users/spatial layers is obtained and propose a mapping function to allocate a specific cyclic shift value to each user; such SU-MIMO channel estimation schemes are also applicable for MU-MIMO. Further, we analyze the trade-off between the channel's delay spread and the number of users for MU-MIMO exploiting a low complexity channel estimation method from our previous work [11] by simulation.

This paper is organized as follows. The LTE-A system models for SU-MIMO and MU-MIMO are introduced in Section II. In Section III the reference symbol allocation and structure is explained. Channel estimation is considered in Section IV. Section V and Section VI contain simulation results and the conclusion, respectively.

II. System Model

The LTE-A uplink employs Single-Carrier Frequency Division Multiplexing (SC-FDM) as physical layer access scheme, which is basically Discrete Fourier Transform (DFT) spread OFDM. This means that modulated symbols of each spatial transmission layer are DFT transformed prior to the MIMO OFDM processing as explained in [12]. Similarly, received

978-1-4673-8999-0/17/$31.00 ©2017 IEEE

symbols are transformed by an Inverse Discrete Fourier Transform (IDFT). Due to this layer-wise spreading, a single carrier like physical layer scheme is obtained, in the sense that each symbol is spread over all subcarriers for transmission. For the purpose of channel estimation however, the system model corresponds to OFDM, since the pilot symbols are multiplexed after the DFT spreading and the channel estimation takes place prior to de-spreading [12]. We consider a perfectly synchronized OFDM transmission with $k \in \{1, \ldots, N_{\mathrm{SC}}\}$ scheduled subcarriers and $n \in \{1, \ldots, 7\}$ OFDM symbols per slot, corresponding to normal Cyclic Prefix (CP) length operation of LTE-A. We assume the wireless channel to be constant for the duration of an OFDM symbol and the CP length to be longer than the channel's delay spread such that no inter-symbol or inter-carrier interference occurs.

A. Single-User MIMO

In SU-MIMO a single user is scheduled exclusively on N_{SC} subcarriers for the duration of a slot, employing N_L spatial layers. The number of layers is at most four since 3GPP LTE-A Rel. 10 and at most equal to the number of transmit antenna ports N_T, i.e., $N_L \leq N_T \leq 4$. We denote the transmit symbols at OFDM symbol time n of all scheduled N_{SC} subcarriers on spatial layer ℓ by vector $\mathbf{x}_{n,\ell} \in \mathcal{A}^{N_{\mathrm{SC}} \times 1}$, where $\mathcal{A}$ denotes the symbol alphabet. Symbol vectors of all layers are stacked into symbol vector $\mathbf{x}_n$ as

$$\mathbf{x}_n = \begin{pmatrix} \mathbf{x}_{n,1} \\ \mathbf{x}_{n,2} \\ \vdots \\ \mathbf{x}_{n,N_L} \end{pmatrix} \in \mathcal{A}^{N_{\mathrm{SC}} N_L \times 1} \ . \tag{1}$$

Further we define a block-wise effective channel matrix at symbol time n as

$$\mathbf{H}_n = \begin{pmatrix} \mathbf{H}_{1,1,n} & \cdots & \mathbf{H}_{1,N_L,n} \\ \vdots & \ddots & \vdots \\ \mathbf{H}_{N_R,1,n} & \cdots & \mathbf{H}_{N_R,N_L,n} \end{pmatrix} , \tag{2}$$

where blocks $\mathbf{H}_{i,\ell,n} \in \mathbb{C}^{N_{\mathrm{SC}} \times N_{\mathrm{SC}}}$ are diagonal matrices consisting of OFDM channel coefficients for N_{SC} scheduled subcarriers from layer $\ell \in \{1, \ldots, N_L\}$ to receive antenna $i \in \{1, \ldots, N_R\}$ at symbol time n. The effective channel (2) includes the precoder $\mathbf{F}'_n \in \mathbb{C}^{N_T N_{\mathrm{SC}} \times N_L N_{\mathrm{SC}}}$ as given by

$$\mathbf{H}_n = \mathbf{H}_n^{(d)} \mathbf{F}'_n \ , \tag{3}$$

where $\mathbf{H}_n^{(d)} \in \mathbb{C}^{N_R N_{\mathrm{SC}} \times N_T N_{\mathrm{SC}}}$ is the block-wise diagonal channel matrix consisting of channel coefficients from all N_T transmit antenna ports to all N_R receive antennas. The precoding matrix is constant over all subcarriers and can therefore be expressed by

$$\mathbf{F}'_n = \mathbf{F}_n \otimes \mathbf{I}_{N_{\mathrm{SC}}} \ , \tag{4}$$

where $\otimes$ denotes the Kronecker product, $\mathbf{I}_{N_{\mathrm{SC}}}$ is the identity matrix of size N_{SC} and $\mathbf{F}_n \in \mathbb{C}^{N_T \times N_L}$. The system model in vector notation is given by

$$\mathbf{y}_n = \mathbf{H}_n \mathbf{x}_n + \mathbf{z}_n \ , \tag{5}$$

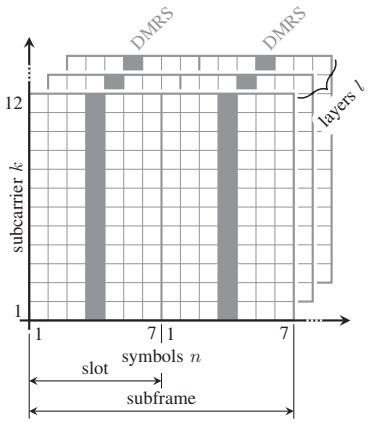

Fig. 1. Reference symbol allocation.

with the independent and identically distributed Gaussian noise vector $\mathbf{z}_n \sim \mathcal{CN}\left(0, \sigma_z^2 \mathbf{I}_{N_R N_{\mathrm{SC}}}\right)$.

B. Multi-User MIMO

For MU-MIMO transmission we assume N_u scheduled users that are assigned the same N_{SC} subcarriers within a slot. Further, all UEs are equipped with a single transmit antenna port each, enabling transmissions on a single spatial layer only. Modulated symbols at OFDM symbol time n, for all N_{SC} subcarriers of user u are described by vector $\mathbf{x}_{n,u} \in \mathcal{A}^{N_{\mathrm{SC}} \times 1}$. Stacking data vectors from all scheduled users $u \in \{1, \ldots, N_u\}$ yields the symbol vector

$$\mathbf{x}_n = \begin{pmatrix} \mathbf{x}_{n,1} \\ \mathbf{x}_{n,2} \\ \vdots \\ \mathbf{x}_{n,N_u} \end{pmatrix} \in \mathcal{A}^{N_{\mathrm{SC}} N_u \times 1} \ , \tag{6}$$

similar to (1). For MU-MIMO the block-wise diagonal channel matrix at symbol time n is given by

$$\mathbf{H}_n = \begin{pmatrix} \mathbf{H}_{1,1,n} & \cdots & \mathbf{H}_{1,N_u,n} \\ \vdots & \ddots & \vdots \\ \mathbf{H}_{N_R,1,n} & \cdots & \mathbf{H}_{N_R,N_u,n} \end{pmatrix} , \tag{7}$$

which is very similar to (2) except the number of layers is exchanged by the number of single layer users N_u [13]. A stacked system model for MU-MIMO then follows the same formalism (5).

For SU-MIMO operation, symbols $\mathbf{x}_n$ and channel matrix $\mathbf{H}_n$ are given by (1) and (2), respectively, while they are given by (6) and (7), respectively for MU-MIMO operation.

III. Reference Symbols

Channel estimation in LTE-A is pilot aided with reference symbols as defined in [1]. Since DMRS of all users and all spatial transmission layers are allocated on the same time-frequency resources, estimated channels need to be separated by utilizing the DMRS code domain orthogonality at the receiver. In this section we briefly introduce DMRS in the

TABLE I
DEPENDENCE OF $n^{(2)}_{\mathrm{DMRS},\ell,S}$ ON LAYER ℓ AND CSF S.

S	$n^{(2)}_{\mathrm{DMRS},\ell,S}$			
	ℓ=1	ℓ=2	ℓ=3	ℓ=4
0	0	6	3	9
1	6	0	9	3
2	3	9	6	0
3	4	10	7	1
4	2	8	5	11
5	8	2	11	5
6	10	4	1	7
7	9	3	0	6

context of MU-MIMO Channel Estimation (CE); further details can be found in [14]–[16].

DMRS are multiplexed in time with the transmit data at OFDM symbol time $n = 4$ in every slot and on the entire scheduled transmission bandwidth, of N_{SC} subcarriers as shown in Fig. 1. Since reference symbols are always allocated at the same symbol time, we omit the symbol time index n in the following. The pilot sequences consist of a base sequence and a cyclic shift. The base sequence of a DMRS on N_{SC} subcarriers for one slot is denoted by $\bar{\mathbf{r}} \in \mathbb{C}^{N_{\mathrm{SC}}\times 1}$. It is a complex exponential sequence, lying on the unit circle and therefore fulfills

$$|\bar{\mathbf{r}}[k]| = 1 \qquad \forall k \in \{1,\ldots,N_{\mathrm{SC}}\} \tag{8}$$

where square brackets $[\cdot]$ denote the vector entry.

DMRS for one slot are defined by [5] the diagonal matrix

$$\mathbf{R}^S_\ell = \mathbf{T}^S_\ell \,\mathrm{Diag}\,(\bar{\mathbf{r}}) \in \mathbb{C}^{N_{\mathrm{SC}}\times N_{\mathrm{SC}}} \ , \tag{9}$$

with layer index ℓ and CSF S. The cyclic shift operator is given by

$$\mathbf{T}^S_\ell = \mathrm{Diag}\left(e^{j0},\ldots,e^{j\alpha^S_\ell(k-1)},\ldots,e^{j\alpha^S_\ell(N_{\mathrm{SC}}-1)}\right) \ , \tag{10}$$

where the operator $\mathrm{Diag}(\cdot)$ yields a diagonal matrix from a vector. The cyclic shift value α^S_ℓ depends on the spatial layer index ℓ and the CSF S from uplink related DCI format. It is defined by [1]

$$\alpha^S_\ell = \frac{2\pi n_{\mathrm{cs},\ell,S}}{12} \tag{11}$$

with

$$n_{\mathrm{cs},\ell,S} = \left(n^{(1)}_{\mathrm{DMRS}} + n^{(2)}_{\mathrm{DMRS},\ell,S} + n_{\mathrm{PN}}\right) \bmod 12 \ . \tag{12}$$

The only layer dependent term in (12) is $n^{(2)}_{\mathrm{DMRS},\ell,S}$ since $n^{(1)}_{\mathrm{DMRS}}$ is given by higher network layers and n_{PN} is a pseudo-random sequence. This value is signaled in terms of the uplink related DCI format, in which a field of three bits is reserved for this purpose, namely the CSF [1], [17]. The relation between this CSF from DCI signalling and $n^{(2)}_{\mathrm{DMRS},\ell,S}$ is given by Table I which originates from Table 5.5.2.1.1-1 in [1]. As the cyclic shift explicitly depends on the transmission layer index ℓ as well as on the signaled CSF value S, orthogonality between pilots can be obtained for SU-MIMO and for MU-MIMO transmissions.

Due to the intended pilot sequence orthogonality, the inner product of two DMRS is the factor, determining the inter-layer interference for correlation based estimation. It is therefore crucial to analyse how the Frequency Domain Code Division Multiplexing (FD-CDM) orthogonality can be exploited in order to cancel this interference. Exploiting (8), the product of two DMRS from layers ℓ and p with $\ell, p \in \{1,\ldots,N_L\}$ and CSFs S and C, becomes

$$\begin{aligned}\left(\mathbf{R}^S_\ell\right)^H \mathbf{R}^C_p &= \left(\mathbf{T}^S_\ell\right)^H \mathbf{T}^C_p \,\mathrm{Diag}\,(\bar{\mathbf{r}})^H \,\mathrm{Diag}\,(\bar{\mathbf{r}}) \\ &= \mathrm{Diag}\Big(e^{j0},\ldots,e^{j\Delta\alpha(k-1)},\ldots,e^{j\Delta\alpha(N_{\mathrm{SC}}-1)}\Big)\mathbf{I} \ ,\end{aligned} \tag{13}$$

with $\Delta\alpha = \alpha^C_p - \alpha^S_\ell$ being the cyclic phase shift between DMRS of two different spatial layers $p \neq \ell$ or users that are assigned two different CSF $C \neq S$. The exponential sequence (13) therefore has a periodicity of $\gamma = 2\pi/\Delta\alpha$. The FD-CDM orthogonality can be exploited as

$$\mathrm{trace}\left(\left(\mathbf{R}^C_p\right)^H \mathbf{R}^S_\ell\right) = \begin{cases} N_{\mathrm{SC}} & \text{for } p=\ell \text{ and } C=S \\ 0 & \text{for } p\neq\ell \text{ or } C\neq S \end{cases} \ . \tag{14}$$

Since the phase shift $\Delta\alpha$ is a fraction of 12 trough (11) and the number of subcarriers N_{SC} is a multiple of 12 in LTE-A, summation over the whole exponential sequence evaluates to zero in (14) for two different layers or users. After transmission over a frequency selective channel, this orthogonality has to be exploited to separate all effective MIMO channels at the receiver.

For SU-MIMO, correlation of the received signal of layer p with reference symbol of intended layer ℓ to be estimated leads to inter-layer interference. The structure of this interference was analyzed in (13), where the cyclic shift $\Delta\alpha$ depends on the two layers p and ℓ. For correlation based estimation, the cyclic shift value is a distance measure between MIMO channels and directly affects their separability. As all pairings $p \neq \ell$ occur, the minimum cyclic shift $\Delta\alpha_{\min}$ between any two layers determines the residual error floor for correlation based estimation. For a SU-MIMO transmission, i.e., $N_L > 1$, this minimum difference in cyclic shift is given by

$$\Delta\alpha_{\min} = \min_{\substack{p,\ell\in\{1,\ldots,N_L\}\\ p\neq\ell}} |\Delta\alpha| \ , \tag{15}$$

which corresponds to a maximum periodicity $\check{\gamma} = 2\pi/\Delta\alpha_{\min}$.

In case of a MU-MIMO transmission, similar effects occur. Code domain orthogonality is then exploited between two CSF values C and S, corresponding to two users j and u, such that (14) is again applicable. Applying this change of indices to (15), a minimum cyclic shift value is also found for MU-MIMO transmissions.

A. The Single-User MIMO Case

In a SU-MIMO scenario only one user is scheduled per time-frequency resource. This scheduled user transmits on N_L spatial transmission layers to achieve high spectral efficiency via spatial multiplexing. To estimate the complete MIMO channel, orthogonality between DMRS of the active spatial

TABLE II
RELATION BETWEEN USER INDEX u AND THE CSF.

u	$\Gamma(u)$		$\hat{\Gamma}(u)$	
	S	$n^{(2)}_{\mathrm{DMRS},1,S}$	S	$n^{(2)}_{\mathrm{DMRS},1,S}$
1	0	0	0	0
2	1	6	4	2
3	2	3	3	4
4	7	9	1	6
5			5	8
6			6	10
7			2	3
8			7	9

layers, originating from a single UE, has to be ensured. For this the layer dependence of the cyclic shift (11) is utilized. Assuming a single user transmitting on several spatial layers, only one row, corresponding to the CSF of that specific user, of Table I is relevant. Still, since each layer is assigned a different cyclic shift accordingly, (13) is exploited for CE and evaluates to zero for any two different employed layers $p \neq \ell$.

B. The Multi-User MIMO Case

When MU-MIMO is employed, a certain number of N_u users is scheduled on the same time-frequency resource. For coherent detection channels from all UEs to the Base Station (BS) have to be estimated. This again requires orthogonality between pilot symbols of all spatial layers. However, in MU-MIMO this means orthogonality between DMRS of spatial streams originating from different users rather than from just a single user, as in the SU-MIMO case. For this the dependence of cyclic shift (11) on the signaled CSF S is utilized. When multiple users are transmitting, each employing a single spatial stream, only the first column of Table I is being considered. Since now each UE only utilizes one layer, different cyclic shifts have to be obtained by CSF signaling.

We propose a user index to CSF mapping $S = \Gamma(u)$ as given in Table II. When this mapping is employed, cyclic shifts between different users in the MU-MIMO case are the same as between different layers in the SU-MIMO case. Therefore, all channel estimation methods proposed for SU-MIMO operation are again applicable to MU-MIMO with $N_u \leq 4$, with our introduced mapping function. Since the CSF is a three bit field within DCI signaling, a maximum of $N_u = 8$ is possible for Multi-User (MU) operation. For a number of users $5 \leq N_u \leq 8$ however, a different mapping function $\hat{\Gamma}(u)$ is employed, since it yields higher differences in cyclic shifts between users compared to $\Gamma(u)$. The mapping $\hat{\Gamma}(u)$ is also given in Table II.

IV. CHANNEL ESTIMATION

Considering the received signal of antenna i from (5) for the case of MU-MIMO, yields

$$\mathbf{y}_i = (\mathbf{H}_{i,1}, \ldots, \mathbf{H}_{i,N_u}) \begin{pmatrix} \mathbf{x}_1 \\ \vdots \\ \mathbf{x}_{N_u} \end{pmatrix} + \mathbf{z}_i \ , \tag{16}$$

where the time index n is again omitted. Since channel matrices in (16) are diagonal, channel vectors $\mathbf{h}_{i,u} = \mathrm{diag}\left(\mathbf{H}_{i,u}\right)$ can be exploited instead, where the operator $\mathrm{diag}(\cdot)$ yields a column vector from a diagonal matrix. Further, substituting data symbols by reference symbols (9) yields a model for CE

$$\begin{aligned} \mathbf{y}_i &= \left(\mathbf{R}_1^{\Gamma(1)}, \ldots, \mathbf{R}_1^{\Gamma(N_u)}\right) \begin{pmatrix} \mathbf{h}_{i,1} \\ \vdots \\ \mathbf{h}_{i,N_u} \end{pmatrix} + \mathbf{z}_i \\ &= \sum_{u=1}^{N_u} \mathbf{R}_1^{\Gamma(u)} \mathbf{h}_{i,u} + \mathbf{z}_i \ , \end{aligned} \tag{17}$$

where the layer index is always one, since each user only applies a single spatial stream. Please note that in (17) the CSF index S of reference symbols from (9) is obtained by employing the mapping function $\Gamma(u)$. Applying a least squares estimator for channel $\mathbf{h}_{i,u}$ on (17) as in [11] leads to

$$\begin{aligned} \tilde{\mathbf{h}}_{i,u} &= \left(\mathbf{R}_1^{\Gamma(u)}\right)^H \mathbf{y}_i \\ &= \mathbf{h}_{i,u} + \sum_{\substack{j=1 \\ j \neq u}}^{N_u} \left(\mathbf{R}_1^{\Gamma(j)}\right)^H \mathbf{R}_1^{\Gamma(u)} \mathbf{h}_{i,u} + \left(\mathbf{R}_1^{\Gamma(u)}\right)^H \mathbf{z}_u \ , \end{aligned} \tag{18}$$

where (13) was exploited. As the received signal is multiplied with the reference symbol as initial step in (18), this estimation is also referred to as correlation based estimation.

Considering SU-MIMO operation, an expression similar to (18) is obtained for the estimated channel from spatial transmit layer ℓ to receive antenna i which is given by

$$\tilde{\mathbf{h}}_{i,\ell} = \mathbf{h}_{i,\ell} + \sum_{\substack{j=1 \\ j \neq \ell}}^{N_L} \left(\mathbf{R}_j^{\Gamma(1)}\right)^H \mathbf{R}_\ell^{\Gamma(1)} \mathbf{h}_{i,\ell} + \left(\mathbf{R}_\ell^{\Gamma(1)}\right)^H \mathbf{z}_\ell \ . \tag{19}$$

Since in (18) all N_u users employ a single layer only, the layer index in (18) is fixed to one, i.e., $\ell = 1$. In (19) on the other hand, a single user employs N_L spatial transmit layers such that the user index is fixed to one, i.e., $u = 1$.

As the inter-user or inter-layer interference is characterized by exponential sequences of a maximum periodicity $\check{\gamma} = 2\pi/\Delta\alpha_{\min}$, applying a sliding averaging on (18) or (19) as post-processing yields a channel estimate which significantly reduces interference as proposed in [11]. For this method, we assume the channel to be almost frequency flat over $\check{\gamma}$ subcarriers. The estimate is then obtained by

$$\hat{\mathbf{h}}_{i,\ell}[k] = \frac{1}{\check{\gamma}^2} \sum_{t=k-\check{\gamma}+1}^{k} \sum_{j=t}^{t+\check{\gamma}-1} \tilde{\mathbf{h}}_{i,\ell}[j] \text{ for } \check{\gamma} \leq k \leq N_{\mathrm{SC}} - \check{\gamma} + 1 \ , \tag{20}$$

which is given for SU-MIMO here and the MU-MIMO version is obtained by exchanging layer index ℓ by user index u.

V. SIMULATION RESULTS

Numerical simulations presented in this section were performed with the Vienna LTE-A uplink link level simulator [12], [18], [19]. We show results in terms of channel estimation Mean Square Error (MSE) and resulting Bit Error

Ratio (BER) for a 16QAM symbol alphabet and Minimum Mean Square Error (MMSE) equalization. We exploit (20) for estimation, which we refer to as *averaging* in the following. A bandwidth of $1.4\,\mathrm{MHz}$, which corresponds to $N_{\mathrm{SC}} = 72$, was used for all simulations. With a block-fading assumption the wireless channel is constant in time for a duration of a subframe (two slots). The two channel estimates obtained from these two slots are then averaged for noise reduction and repeated for all OFDM symbol times within a subframe, to obtain channel estimates also on data positions.

SU-MIMO simulation results for a two layer and a four layer transmission with a corresponding number of antennas, i.e., $N_T = N_R = N_L$, are shown in terms of MSE in Fig. 2. A Typical Urban (TU) channel model [20] with a Root Mean Square (RMS) delay spread of $0.5\,\mu\mathrm{s}$ and precoding matrices $\mathbf{F} = 1/\sqrt{N_L}\mathbf{I}_{N_L}$ are utilized. The performance of MMSE estimation with perfectly known second order statistics for two spatial layers is also shown as reference. As channel estimation is performed for each receive antenna individually, same results are obtained for different N_R. Further, as the effective channel, including the precoder, of dimension $N_R \times N_L$ is estimated, the number of transmit antennas N_T has no impact on the obtained MSE. Results show that the estimation error obtained with two active spatial layers is higher compared to four active spatial layers at low Signal to Noise Ratio (SNR), as the received signal is averaged over more subcarriers in the latter case which leads to superior noise reduction. In the high SNR region, the estimation MSE is dominated by the inter-layer interference, leading to a higher error for $N_L = 4$.

Simulation results for MU-MIMO transmissions with different numbers of single transmit antenna port users are shown in Fig. 3. Again, a TU channel model was exploited and numbers of receive antennas were chosen corresponding to the number of users, i.e., $N_u = N_R = \{2, 4, 6, 8\}$. Performance obtained with MMSE estimation for $N_u = 8$ is shown as reference. Similar effects as for SU-MIMO are observed. Again estimation MSE decreases significantly with the number of users at low SNR. Since BER is generally high in this region of low SNR, this improvement in MSE only translates to small improvements in terms of BER. In the high SNR region, interference on a frequency selective channel, which is now inter-user interference, is even more pronounced than in the SU-MIMO case. Comparing Fig. 2 and Fig. 3a, the MU-MIMO MSE curve for $N_u = 2$ is similar to the SU-MIMO MSE curve obtained for $N_L = 2$, the MSE obtained with $N_u = 4$ is already significantly higher than the MSE obtained with $N_L = 4$. The origin of this effect lies in the transmit power. Each user transmits with a normalized power of one for MU-MIMO operation, while the total power of a single user in SU-MIMO is also one, and hence the per-layer power is $1/N_L$. The total power for MU-MIMO transmissions is therefore higher by a factor N_u. This leads to stronger interference resulting in a high estimation MSE floor. The discussed residual channel estimation error at high SNR also leads to a high BER as shown in Fig. 3b.

To investigate the effect of the wireless channel's delay

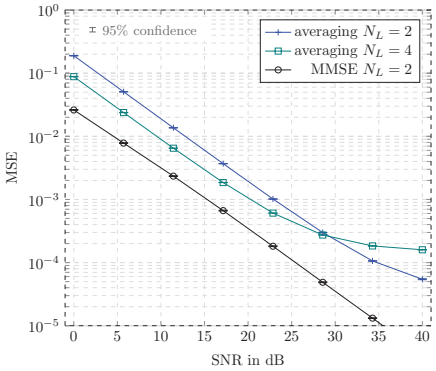

Fig. 2. Results for SU-MIMO on a TU channel model.

spread, i.e., the frequency selectivity, and the number of active users N_u on the channel estimation error, simulations on a channel with exponential power delay profile were carried out. Channel estimation MSE for different RMS delay spreads τ with $N_u = 4$ active users is shown in Fig. 4. The curve for $\tau = 0.5\,\mu\mathrm{s}$ is comparable to the four user case in Fig. 3a which is obtained on a TU channel which also has an RMS delay spread of $0.5\,\mu\mathrm{s}$. It is obvious that inter-user interference cancellation is more difficult on highly frequency selective channels. Since the minimum cyclic shift difference (15) decreases with N_u, the maximum periodicity of interference $\check{\gamma}$ increases. Therefore, serving more users requires a frequency flat channel because the correlation based frequency-domain estimation method (20) assumes the channel to be frequency flat over $\check{\gamma}$ subcarriers. In other words, the residual estimation error for correlation based estimation increases with the number of scheduled users and the RMS delay spread. Although we showed this trade-off in the context of frequency domain estimation, the effect is similar for more common time domain channel estimation.

VI. Conclusion

In this work we showed that the problem of channel estimation is equivalent for SU-MIMO and MU-MIMO in LTE-A uplink. In both cases, reference symbols originating from different spatial layers or users overlap entirely in time and frequency, according to their standardized allocation. Therefore the DMRS code domain orthogonality needs to be exploited to separate MIMO channels at the receiver. We showed that orthogonality can be ensured in between spatial layers of a single users as well as in between multiple users transmitting simultaneously by means of signaling. We proposed a standard compliant mapping function for signaling the CSF to users in MU-MIMO such that reference symbols of users are not only orthogonal, but also SU-MIMO estimation schemes are directly applicable. Since orthogonality is in general destroyed during transmission over a frequency selective channel, the channels RMS delay spread leads to a residual channel estimation error for correlation based estimation. We further analyzed the trade-off between the channel's frequency selectivity and the number of active MU-MIMO users. On a highly frequency

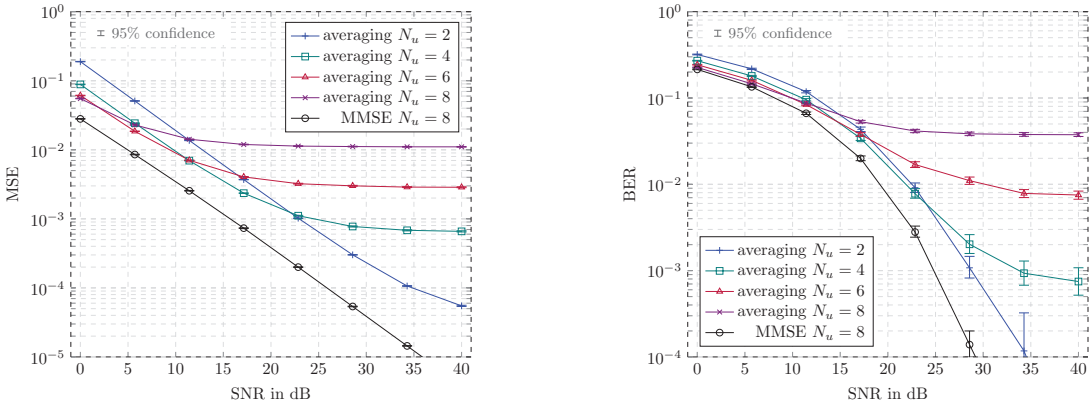

(a) (b)

Fig. 3. MU-MIMO simulation results on a TU channel model in terms of (a) MSE and (b) BER.

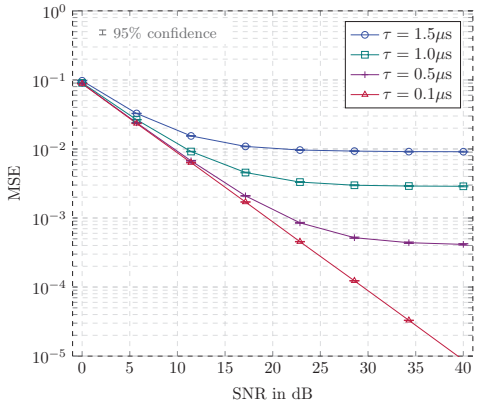

Fig. 4. Results for MU-MIMO with $N_u = 4$ on a channel model with exponential power delay profile and various RMS delay spreads.

selective channel only few users can be served with correlation based estimation without any prior channel statistics.

Acknowledgment

This work has been funded by A1 Telekom Austria AG and the Institute of Telecommunications, TU Wien. The financial support by the Austrian Federal Ministry of Science, Research and Economy and the National Foundation for Research, Technology and Development is gratefully acknowledged.

References

[1] 3rd Generation Partnership Project (3GPP), "Evolved Universal Terrestrial Radio Access (E-UTRA) physical channels and modulation," 3rd Generation Partnership Project (3GPP), TS 36.211, Dec. 2015.

[2] F. Liu, H. Wei, H. Zhao, and Y. Tang, "A novel channel estimation for MIMO SC-FDMA systems," in *IEEE International Conference on Communications, Circuits and Systems (ICCCAS)*, vol. 1, 2013, pp. 96–99.

[3] M. Zhou, B. Jiang, T. Li, W. Zhong, and X. Gao, "DCT-based channel estimation techniques for LTE uplink," in *IEEE 20th International Symposium on Personal, Indoor and Mobile Radio Communications*, 2009, pp. 1034–1038.

[4] H. Sahlin and A. Persson, "Aspects of MIMO channel estimation for LTE uplink," in *IEEE Vehicular Technology Conference (VTC Fall)*, Sep. 2011, pp. 1–5.

[5] C.-Y. Chen and D. Lin, "Channel estimation for LTE and LTE-A MU-MIMO uplink with a narrow transmission band," in *IEEE International Conference on Acoustics, Speech and Signal Processing (ICASSP)*, May 2014, pp. 6484–6488.

[6] Q. Li, Y. Wu, S. Feng, P. Zhang, L. Xue, and Y. Zhou, "On channel estimation for multi-user MIMO in LTE-A uplink," in *IEEE 79th Vehicular Technology Conference (VTC Spring)*, 2014, pp. 1–5.

[7] Z. Rong and G. Fettweis, "Multi-user channel estimation for interference mitigation in the LTE-Advanced uplink," in *IEEE 72nd Vehicular Technology Conference Fall (VTC 2010-Fall)*, 2010, pp. 1–5.

[8] R. Narasimhan and S. Cheng, "Channel estimation and co-channel interference rejection for LTE-Advanced MIMO uplink," in *IEEE Wireless Communications and Networking Conference (WCNC)*, 2012, pp. 416–420.

[9] M. Zhou, B. Jiang, W. Zhong, and X. Gao, "Efficient channel estimation for LTE uplink," in *IEEE International Conference on Wireless Communications & Signal Processing (WCSP)*, 2009, pp. 1–5.

[10] X. Xia, H. Zhao, and C. Zhang, "Improved SRS design and channel estimation for LTE-Advanced uplink," in *IEEE 5th International Symposium on Microwave, Antenna, Propagation and EMC Technologies for Wireless Communications (MAPE)*, Oct. 2013, pp. 84–90.

[11] S. Pratschner, E. Zöchmann, and M. Rupp, "Low complexity estimation of frequency selective channels for the LTE-A uplink," *IEEE Wireless Communications Letters*, vol. 4, no. 6, pp. 673–676, 2015.

[12] E. Zöchmann, S. Schwarz, S. Pratschner, L. Nagel, M. Lerch, and M. Rupp, "Exploring the physical layer frontiers of cellular uplink," *EURASIP Journal on Wireless Communications and Networking*, vol. 2016, no. 1, pp. 1–18, 2016.

[13] L. Nagel, S. Pratschner, S. Schwarz, and M. Rupp, "Efficient multi-user MIMO transmissions in the LTE-A uplink," in *International Workshop on Link- and System Level Simulations (IWSLSS)*, Jul. 2016.

[14] X. Hou, Z. Zhang, and H. Kayama, "DMRS design and channel estimation for LTE-Advanced MIMO uplink," in *IEEE 70th Vehicular Technology Conference Fall (VTC 2009-Fall)*, Sep. 2009, pp. 1–5.

[15] E. Kasem and J. Prokopec, "The evolution of LTE to LTE-Advanced and the corresponding changes in the uplink reference signals," *Elektrorecvue, ISSN*, pp. 1213–1539, 2012.

[16] X. Zhang and Y. Li, "Optimizing the MIMO channel estimation for LTE-Advanced uplink," in *IEEE International Conference on Connected Vehicles and Expo (ICCVE)*, Dec. 2012, pp. 71–76.

[17] E. Dahlman, S. Parkvall, and J. Sköld, *4G: LTE/LTE-advanced for mobile broadband*. Academic press, 2013.

[18] M. Rupp, S. Schwarz, and M. Taranetz, *The Vienna LTE-Advanced Simulators: Up and Downlink, Link and System Level Simulation*, 1st ed., ser. Signals and Communication Technology. Springer Singapore, 2016.

[19] [Online]. Available: http://www.nt.tuwien.ac.at/ltesimulator/

[20] 3rd Generation Partnership Project (3GPP), "Universal Mobile Telecommunications System (UMTS) Deployment aspects," 3rd Generation Partnership Project (3GPP), TR 25.943, Feb. 2010.